

# Design, development, and performance analysis of a magnetorheological damper for piping vibration control

Sandesh Solepatil<sup>1\*</sup> , Amol Mali<sup>1</sup>, Vikas Dive<sup>1</sup>, Aniket Kolekar<sup>1</sup>

<sup>1</sup> Department of Mechanical Engineering, DY Patil International University, Akurdi, Pune, 411044, Maharashtra, India  
\* Corresponding author's e-mail: sandeshpatil310@gmail.com

## ABSTRACT

A magnetorheological (MR) damper is a type of smart device that utilizes magnetorheological fluids – fluids whose viscosity can be altered by an applied magnetic field. A simple design is provided by a MR damper, which consists of MR fluid, magnetic coils, and a hydraulic cylinder. In addition to being easy to construct and controllable in the field, MR dampers have several other benefits, including a relatively low power input need, the capacity to generate high yield stress up to 100 kPa, and stable operation over a broad temperature range (-40 °C to 150 °C). While MR silencers are designed to function between -40 °C and 150 °C, their effectiveness in specific scenarios may be influenced by additional factors beyond the operational limits of the MR fluid alone. MR fluids are also non-toxic and impervious to contaminants. The MR damper can operate as a traditional passive dashpot in fail-safe mode when there is no magnetic field. Due to these advantages, MR dampers are becoming increasingly popular in a variety of applications, such as knee prosthesis, big bridge vibration control, automotive suspensions, and seismic vibration mitigation. The performance of the developed damper is compared to a standard MR damper to determine the optimal blend for vibration attenuation. Understanding the nonlinear hysteretic behavior of an MR damper is essential for effective control under an applied magnetic field. In present work magnetorheological damper is designed, built, and tested for piping vibration having load carrying capacity of 1910 N and its transmissibility for various blends of MR fluid with percentage 40%, 45% and 50% (by weight of oil in damper) is observed and corresponding transmissibility of damper is compared with standard magnetorheological damper.

**Keywords:** MR fluid, operating modes of damper, magnetic circuit, speed, transmissibility of damper.

## INTRODUCTION

Magnetorheological (MR) dampers have been extensively studied for their ability to provide tunable damping through the application of a magnetic field. Recent research has focused on optimizing their design, improving control strategies, and expanding their applications in various domains such as structural engineering, vehicle suspensions, biomedical devices, and offshore platforms. This literature review summarizes recent advancements in MR damper technology based on ten selected studies. Smith et al. (2021) developed and experimentally evaluated a novel MR damper with an improved dynamic range. The study focused on improving the damper's force output and response time by

optimizing the magnetic circuit and fluid flow channel. Their findings demonstrated that the proposed MR damper exhibited a significantly wider range of damping forces compared to conventional designs, making it suitable for applications requiring precise damping control (1). Kumar et al. (2022) investigated adaptive control strategies for vehicle suspension systems utilizing MR dampers. Their research emphasized real-time tuning of damping properties using feedback control mechanisms, which improved ride comfort and vehicle stability. The study concluded that MR dampers outperformed traditional passive suspension systems by offering dynamic adaptability under various road conditions (2). Singh et al. (2022) conducted a comparative study on different control strategies

for MR dampers in vehicle suspension systems. The research analyzed classical controllers, such as PID, alongside modern approaches like fuzzy logic and neural networks. Their findings highlighted that intelligent control methods significantly enhanced the damping performance, optimizing both ride comfort and vehicle handling (3). Lee et al. (2023) explored the effectiveness of MR dampers in seismic performance enhancement of structures. Their study utilized semi-active control strategies to regulate damping forces based on structural motion. Results showed that MR dampers successfully reduced structural responses during seismic events, outperforming conventional damping solutions in energy dissipation and adaptability (4). Nguyen et al. (2023) further expanded on the use of MR dampers for vibration reduction in tall buildings. The study focused on modeling and control approaches, demonstrating that MR dampers provided efficient oscillation suppression in high-rise structures subjected to dynamic forces. Their results emphasized the importance of integrating real-time control algorithms to optimize damping efficiency (5). Chen et al. (2021) investigated the temperature-dependent behavior of MR dampers, analyzing how variations in temperature influenced fluid viscosity and damping performance. Their experimental findings indicated that higher temperatures led to a reduction in MR fluid viscosity, thereby affecting the damping force. The study emphasized the need for thermally stable MR fluids to ensure consistent performance across a wide temperature range (6). Gupta et al. (2022) developed

a compact MR damper for prosthetic knee applications. Their study focused on designing an MR damper that provided smooth and adaptive resistance for knee joint movement. The results demonstrated that the MR-based knee damper significantly improved mobility and comfort for users by allowing real-time adjustment of damping forces based on walking conditions (7).

Kim et al. (2023) explored the use of MR dampers in wearable devices for human motion assistance. Their study integrated MR dampers into exoskeletons and rehabilitation devices, allowing precise control over resistance forces. The research concluded that MR-based wearable devices could enhance mobility and assist individuals with motor impairments by providing adjustable and responsive damping control (8). Martinez et al. (2024) evaluated the performance of MR dampers in offshore platform applications. Their study focused on mitigating wave-induced vibrations in marine structures. Results showed that MR dampers effectively reduced oscillations, improving structural stability in harsh environmental conditions. The study concluded that MR dampers offered a promising solution for enhancing the durability and safety of offshore platforms (9). Zhang et al. (2024) conducted real-time hybrid simulations of structures equipped with MR dampers to assess their behavior under dynamic loading conditions. Their study validated the effectiveness of MR dampers in structural control applications, demonstrating their adaptability in real-time scenarios. The findings provided valuable insights

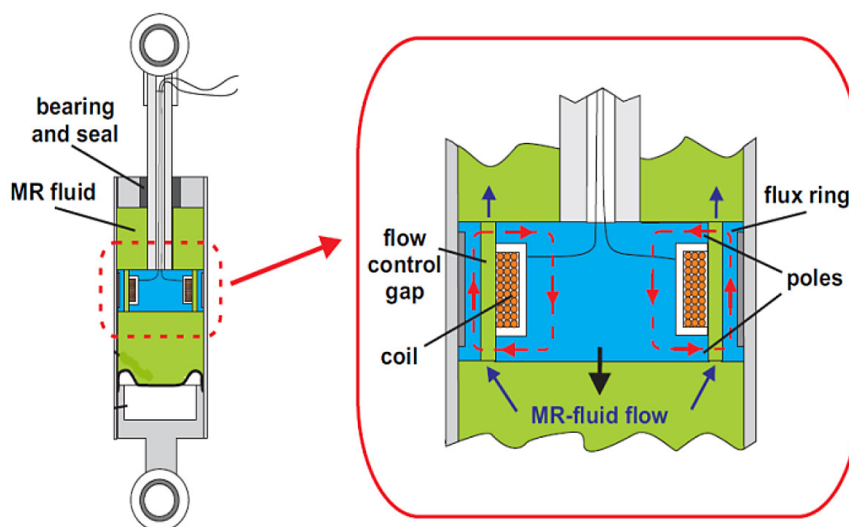


**Figure 1.** Schematic cross-section view of a magneto-rheological Damper

for optimizing MR damper integration in various engineering applications (10).

MR dampers as shown in Figure 1 feature minimal moving parts, relaxed tolerances, and direct interfacing with electronic control systems, making them both reliable and easy to integrate into existing frameworks [6–8]. MR fluids consist of micron-sized ferrous particles suspended in a carrier fluid, typically oil. When exposed to a magnetic field, these particles align along the field lines, significantly increasing the fluid’s viscosity and thereby enhancing its damping capacity (11–12). This controllable behavior allows MR dampers to adjust the damping force in real-time, providing an adaptive response to varying vibration and shock loads (13–14). In recent years, semi-active control devices, such as MR dampers, have gained traction due to their ability to offer the adaptability of active control systems without the need for substantial power resources (15). This makes MR dampers an attractive solution for applications where energy efficiency and adaptability are critical. The design and optimization of MR dampers involve careful consideration of several parameters, with the gap distance between the piston and cylinder being a crucial factor (16–17).

This study explores the performance characteristics of an MR damper prototype, employing various MR fluid blends to evaluate their effectiveness in vibration mitigation. The findings underscore the potential of MR dampers to revolutionize vibration control technologies, providing robust and efficient solutions across multiple domains.

### Parameters affecting performance of MR damper

The performance of MR dampers is influenced by various parameters, both intrinsic to the damper design and external environmental factors. Understanding these parameters is crucial for optimizing the performance of MR dampers in different applications (18).

#### Magnetic field strength

The strength of the magnetic field directly affects the alignment of the iron particles in the MR fluid, thereby altering the fluid’s viscosity and the damping force. Higher magnetic field strengths result in higher damping forces. Precise control of the electromagnetic coil’s current is necessary to adjust the magnetic field strength effectively.

#### MR fluid composition

The properties of the MR fluid, including the type and concentration of iron particles and the carrier fluid, significantly impact the damper’s performance. Smaller or more spherical particles can provide more uniform and predictable changes in viscosity (19). Fluid structure after applying magnetic field is shown in Figure 2.

#### Carrier fluid viscosity

The base viscosity of the carrier fluid affects the range of damping forces that can be achieved.

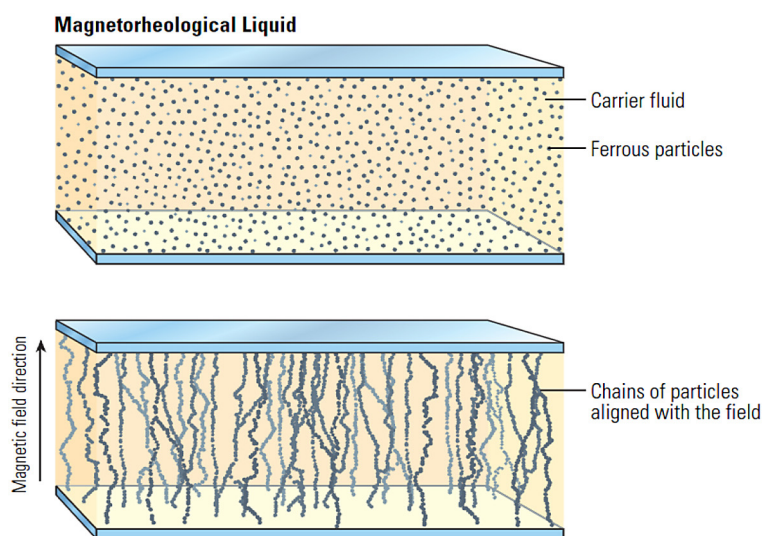


Figure 2. Chain like structure formation in controllable fluid

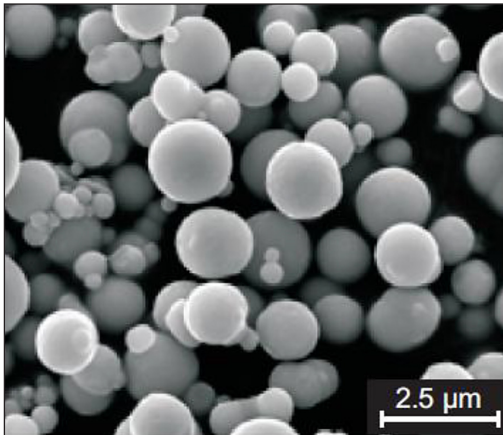


Figure 3. Magnetisable particles in spherical shape

Spherical particle of 2.5  $\mu\text{m}$  is used in MR fluid as shown in Figure 3. In this study, the MR fluid was prepared using iron particles with a specified average diameter of 2.5  $\mu\text{m}$  with a distribution range from 0.2  $\mu\text{m}$  to 4  $\mu\text{m}$ .

### Temperature

Temperature changes can affect the viscosity of the MR fluid and the performance of the electromagnet. Higher temperatures may reduce the fluid’s viscosity, while lower temperatures may increase it. Effective thermal management and the use of temperature-stable MR fluids are essential for consistent performance (20).

### Frequency of excitation

The frequency of the input vibrations or oscillations affects the damper’s response. MR dampers typically perform differently at varying frequencies, and their effectiveness can vary depending on the application. Understanding the frequency range within which the damper needs to operate is crucial for optimal design.

### Damper geometry and design

The physical design of the damper, including the size and shape of the piston, cylinder, and magnetic circuit, influences the distribution and strength of the magnetic field within the damper. The design of the flow path for the MR fluid affects how quickly the fluid can respond to changes in the magnetic field (21).

## Operating modes in magnetorheological damper

MR dampers operate based on the change in the rheological properties of MR fluid in response to a magnetic field. These changes allow the damper to adjust its damping characteristics in real-time. There are three primary operating modes for MR dampers:

### Flow mode

In the flow mode, the MR fluid flows between stationary plates or through a channel. When a magnetic field is applied, the viscosity of the MR fluid increases, causing a higher resistance to flow. This mode is typically used linear dampers where the fluid flow is controlled to vary the damping force as shown in Figure 4.

### Shear mode

In shear mode, the MR fluid is placed between two surfaces that move relative to each other. When a magnetic field is applied, the particles in the MR fluid align along the field lines, increasing the shear stress required to move the surfaces relative to each other. This mode is useful in applications where rotational or torsional forces need to be controlled, such as in rotary dampers or clutches as shown in Figure 5.

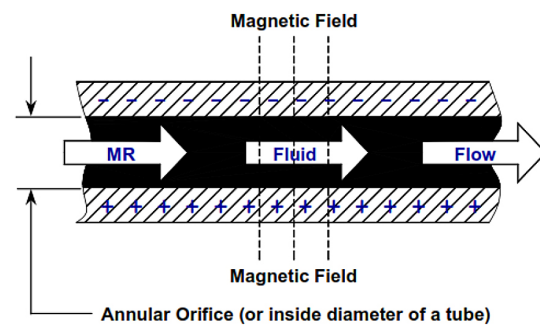


Figure 4. MR fluid used in flow mode

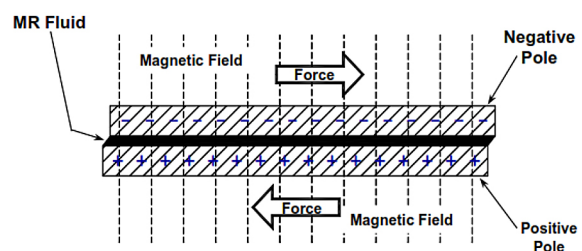


Figure 5. MR fluid used in shear mode

### Squeeze mode

In squeeze mode, the MR fluid is squeezed between two surfaces that move towards or away from each other. The application of a magnetic field changes the resistance to this squeezing motion. This mode is less common than flow and shear modes but can be effective in certain applications where axial or compressive forces are predominant as shown in Figure 6.

Each of these modes allows MR dampers to be highly versatile and adaptable to different applications, such as in automotive suspensions, seismic dampers, prosthetics, and various industrial machinery. The choice of mode depends on the specific requirements of the application, including the type of motion, the range of forces, and the desired level of control.

### Magnetic circuit design

The magnetic circuit of the MR damper consists of the upper piston part, lower piston part, and casing, all of which contribute to the generation and distribution of the magnetic field. The materials and parameters used in its design are as follows:

## MATERIALS

1. Upper piston part – low-carbon steel (e.g., AISI 1010) chosen for its high magnetic permeability and good machinability.
2. Lower piston part – soft magnetic iron ensures efficient magnetic flux conduction with minimal losses.
3. Casing – mild steel or stainless steel provides mechanical strength while allowing magnetic flux flow.
4. Magnetic coil – copper wire (enameled) – used for electromagnetic induction, with high conductivity and heat resistance.
5. MR fluid – a blend of carrier oil (silicone oil or mineral oil) and ferrous particles (iron or iron-based alloys), typically with a weight concentration of 40–50%.

### Parameters

1. Operating current – typically 0.1–2 A, depending on the design and required damping force.
2. Coil turns (N) – optimized based on the required magnetic field strength, 3093 turns.

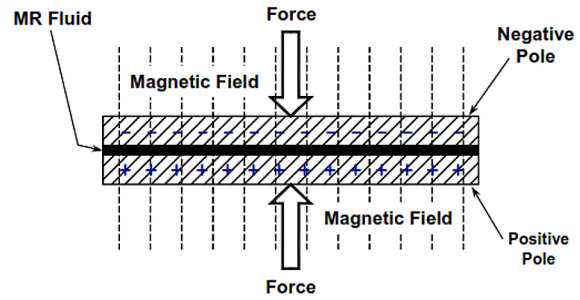


Figure 6. MR fluid used in squeeze mode

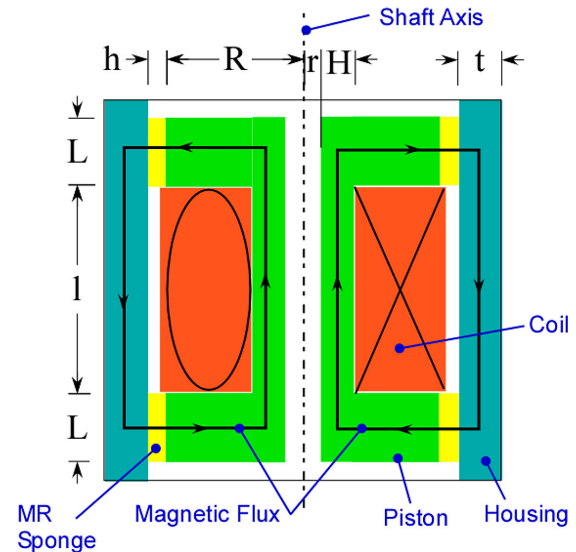


Figure 7. Dimensions of MR fluid damper

The MR damper’s magnetic circuit is made up of the casing, the upper and lower piston parts as shown in Figure 7. A necessary-turn magnetic coil was wound between these parts. When such a material is initially subjected to a magnetic field (H), its magnetic induction (B) increases gradually at first, then more quickly, then very slowly once again, and ultimately reaches a point known as magnetic saturation. Magnetic flux  $\Phi$  and magnetic reluctance  $R_m$  can be used to compute magnetic potential F.

$$F = R_m \times \Phi \tag{1}$$

where:  $F = NI$ ; N is no. of turns and I is max. current.

Total reluctance of the device is given by:

$$R_T = \sum_{i=1}^n \frac{L_i}{\mu A_i} \tag{2}$$

where:  $L_i$ ,  $A_i$ , and  $\mu_i$  are the length, cross sectional area, and permeability of element  $i$  in the magnetic flux path.

$$\Phi = \frac{NI}{R_T} \tag{3}$$

$$B = \frac{\phi}{A} \text{ in Tesla} \quad (4)$$

Magnetic force developed by circuit

$$F = \tau A \quad (5)$$

where:  $\tau$  is shear stress value of MR fluid 45–100 kPa and  $A$  is magnetic flow area.

Magnetic circuit is design with the following dimensions to sustain load of 1800 N. R = 36 mm, H = 10 mm, L=15 mm, l = 40 mm. h = 2 mm, r = 10 mm and t = 4 mm

### Methodology

1. Design of MR fluid damper based on literature survey.
2. Manufacturing of damper.
3. Study detail preparation, compositions of MR fluid.
4. Decide the blending compositions of MR fluid.
5. Test the damper performance on damper test rig for flow gap of 0.5 mm and 2 mm For 2000 N load carrying capacity (Table 1).

### EXPERIMENTAL WORK

A shock absorber test rig is used to verify the functioning of the planned damper a shown in Figure 8. Vibrational force is produced by eccentric mass. The vibrating force grew as the motor speed rose. Mass rotating motion is transformed into linear motion. The damper is tested at different speeds and with different currents (ranging from 0 to 2 A). Using a load cell indicator, the transmitted load is determined. To evaluate the performance and functionality of the designed magnetorheological (MR)

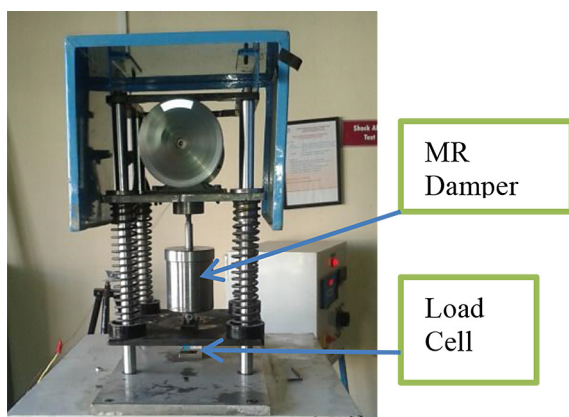


Figure 8. Experimental setup of magnetorheological damper

damper, a shock absorber test rig is used. This setup allows the verification of damping characteristics under various operational conditions, including different speeds and applied currents. The operation speed of motor is taken 0 rpm to 250 rpm based on frequency calculations and current values are 0.1 A to 0.8 A based on calculation of magnetic coil. The testing procedure involves the following key components and steps: The MR damper is mounted on a shock absorber test rig, as shown in Figure 8. This setup is designed to simulate real-world vibrational forces and assess the damper’s response under different conditions

### Test rig specification

#### Motor

- Power: 0.5 kW/0.5 HP,
- Model: S.R,
- Voltage: 180 V,
- Current: 2.5 A,
- Speed: 1500 rpm,
- Serial No: 6/2011,
- Duty cycle: S1.

#### Dimmer

- Current capacity: 2 A,
- Input voltage: 0 to 230 V AC,
- Output voltage: 0 to 270 V AC.

#### RPM indicator

- 4-digit display,
- Make: selectron,
- Model: RC 102 C.

#### Load indicator

- Make: concert electronics,
- Capacity: 0 to 200 kg,
- Resolution: 0.1 kg.

#### Proximity switch

- Make: sai control system,
- Model: PS 13 PNP,
- Supply: 10-30V DC,
- Load capacity: 250,
- Serial No: 110/297.

#### Load cell

- Make: model-C2L30IC,
- Serial No: 055,
- Capacity: 200 kg,
- Accuracy: 0.02% FS.

**Table 1.** Properties of MR fluid

Parameters	MR fluids
Max. yield stress	50–100 kPa
Max. field	~250 kA/m
Viscosity	0.1–1.0 Pa.s
Operable temperature range	-40 to 150 °C (20 °C initial temperature of MR Fluid and final temperature is 75 °C during experiment)
Stability	Unaffected by most impurities
Response time	< millisecond
Density	3–4 g/cm <sup>3</sup>
Power supply	2–25 V at 0–2 A

**Vibration force generation**

- An eccentric mass mechanism is used to generate oscillatory motion.
- The rotating mass produces an increasing vibrational force as the motor speed increases.
- The rotational motion of the mass is converted into linear motion, which directly affects the MR damper.

**Testing parameters**

*Variation in motor speed*

The damper is subjected to different speeds from 0 to 250 rpm to simulate various dynamic conditions. The frequency and amplitude of vibration are adjusted based on the motor speed.

*Current variation (0–2 A)*

The MR damper is tested under different applied currents, ranging from 0 A (passive mode) to 2 A (active mode). As the current increases, the magnetic field strength increases, leading to a higher damping force due to the realignment of MR fluid particles. Damper is tested upto 0.8 A current which is sufficient to generate magnetic field for sustaining force of 1910 N.

*Load measurement*

- A load cell indicator is used to measure the transmitted force through the damper.
- The load cell records the damping force at different test conditions, providing insights into the dynamic behavior of the MR damper.

**Blending of MR fluid**

- Sample 1: In this sample we mixed 40% iron magnetic particles and 60% silicon oil.

- Sample 2: In this sample we mixed 45% iron magnetic particles and 55% silicon oil.
- Sample 3: In this sample we mixed 50% iron magnetic particles and 50% silicon oil.

To compare the transmissibility of present MR damper with standard Lord’s MR damper following experimental procedure is used:

- Testing of different blending 40%, 45% and 50% iron particle to get max. transmissibility reduction in which transmissibility Vs. Speed graph is plotted.
- By increasing speed of rotor frequency (5 Hz) is increased, graph of transmissibility vs frequency is plotted.
- Comparison of transmissibility for present MR damper and standard Lord’s MR damper

**RESULTS AND DISCUSSION**

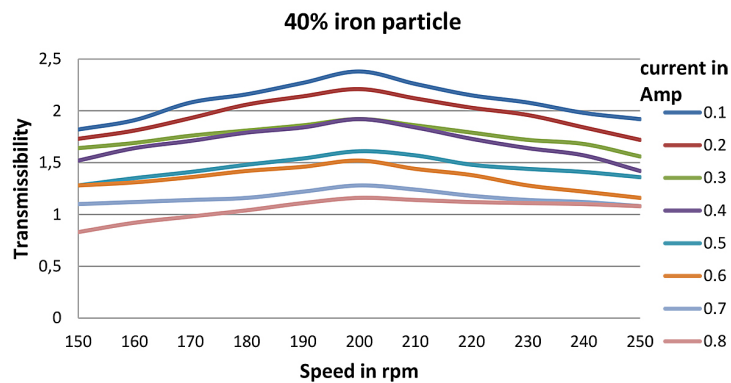
**Results of designed MR damper: SAMPLE 1 (40% iron particle): Transmissibility of damper**

Table 2 provides data on the transmissibility of an MR damper containing a 40% iron particle concentration under different current levels (in amperes) and rotational speeds (in rpm). Transmissibility here likely refers to the ratio of output to input amplitude of vibration, indicating how well the damper can reduce or transmit vibrations.

As the current increases from 0.1 to 0.8 A, the transmissibility values generally decrease at each speed. This indicates that the damper’s ability to reduce vibrations improves with higher current, as the magnetic field strengthens and the MR fluid becomes more viscous, providing greater resistance to motion. At each current level, transmissibility values tend to increase with

**Table 2.** Transmissibility of damper for sample 1

Speed (rpm)	Current (A)							
	0.1	0.2	0.3	0.4	0.5	0.6	0.7	0.8
150	1.82	1.73	1.64	1.52	1.28	1.28	1.1	0.83
160	1.91	1.81	1.69	1.64	1.35	1.31	1.12	0.92
170	2.08	1.93	1.76	1.71	1.41	1.36	1.14	0.98
180	2.16	2.06	1.81	1.79	1.48	1.42	1.16	1.04
190	2.27	2.14	1.86	1.84	1.54	1.46	1.22	1.11
200	2.38	2.21	1.92	1.92	1.61	1.52	1.28	1.16
210	2.26	2.12	1.86	1.84	1.57	1.44	1.24	1.14
220	2.15	2.03	1.79	1.73	1.48	1.38	1.18	1.12
230	2.08	1.96	1.72	1.64	1.44	1.28	1.14	1.11
240	1.98	1.84	1.68	1.57	1.41	1.22	1.12	1.1
250	1.92	1.72	1.56	1.42	1.36	1.16	1.08	1.08



**Figure 9.** Transmissibility v/s speed for sample 1

speed up to a certain point, indicating that higher speeds may reduce the damper’s effectiveness to some extent. However, the effect of speed is less significant compared to the effect of current as shown in Figure 9.

The combination of higher current and lower speed generally results in the lowest transmissibility values, indicating optimal damping performance. For example, at 150 rpm and 0.8 A, the transmissibility is 0.83, which is the lowest value in the Table 2.

At higher speeds (e.g., 250 rpm), even with increased current, the transmissibility does not decrease as significantly, highlighting the challenge of damping at higher operational speeds.

**SAMPLE 2 (45% iron particle): Transmissibility of damper**

Table 3 provides data on the transmissibility of an MR damper at various currents and speeds. Transmissibility in this context refers to the ratio of the output to input amplitude of vibration,

which indicates the damper’s effectiveness in reducing vibrations. Lower transmissibility values suggest better damping performance.

As the current increases from 0.1 to 0.8 amps, the transmissibility values generally decrease at each speed. This trend indicates that the damper’s effectiveness in reducing vibrations improves with higher current. The magnetic field strengthens, increasing the viscosity of the MR fluid and enhancing the damping force. At each current level, transmissibility values tend to increase with speed up to a certain point. Higher speeds typically reduce the damper’s effectiveness, but this effect can be moderated by increasing the current. The combination of higher current and lower speed generally results in the lowest transmissibility values, indicating optimal damping performance. For example, at 150 rpm and 0.8 A, the transmissibility is 0.78, which is among the lowest values in the table. At higher speeds (e.g., 250 rpm), the transmissibility values are still lower at higher currents, but the reduction

**Table 3.** Transmissibility of damper for sample 2

Speed (rpm)	Current (A)							
	0.1	0.2	0.3	0.4	0.5	0.6	0.7	0.8
150	1.84	1.76	1.52	1.44	1.12	0.91	0.78	0.78
160	1.91	1.84	1.61	1.52	1.32	0.96	0.84	0.86
170	1.98	1.99	1.69	1.64	1.44	1.02	0.91	0.94
180	2.07	2.04	1.73	1.72	1.54	1.06	0.96	0.98
190	2.18	2.11	1.76	1.76	1.66	1.12	1.04	1.06
200	2.29	2.16	1.82	1.82	1.74	1.18	1.12	1.12
210	2.12	2.04	1.74	1.68	1.62	1.14	1.08	1.06
220	2.03	1.92	1.68	1.64	1.48	1.09	1.02	1.02
230	1.92	1.84	1.53	1.51	1.42	1.06	0.96	0.96
240	1.86	1.72	1.44	1.42	1.36	1.02	0.92	0.92
250	1.81	1.61	1.39	1.36	1.24	0.96	0.86	0.84

is less pronounced compared to lower speeds. The MR damper’s performance improves significantly with increasing current, as shown by the decreasing transmissibility values across all speeds as shown in Figure 10.

While speed affects transmissibility, its impact is less significant than that of the current. Higher speeds generally lead to higher transmissibility values, but this effect can be mitigated by applying higher currents. The best damping performance (lowest transmissibility) is achieved at the highest current (0.8 A) and lower speeds (150 rpm).

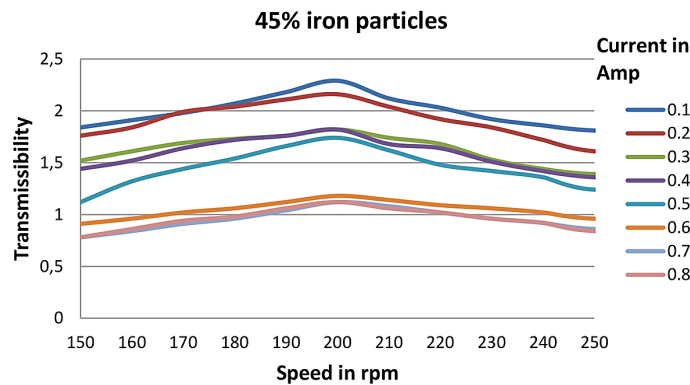
**SAMPLE 3 (50% iron particle): Transmissibility of damper**

Table 4 presents the transmissibility of an MR damper containing a 50% iron particle concentration at various current levels and rotational speeds. Transmissibility here refers to the ratio of the output to input amplitude of vibration,

with lower values indicating better damping performance.

As the current increases from 0.1 to 0.8 amps, the transmissibility values generally decrease at each speed, indicating improved damping performance with higher current. At 150 rpm, the transmissibility drops from 1.86 at 0.1 A to 0.62 at 0.8 A, showing a significant improvement in vibration reduction.

At each current level, transmissibility values tend to increase with speed up to a certain point, suggesting that higher speeds generally reduce the damper’s effectiveness. At 0.1 A, transmissibility increases from 1.86 at 150 rpm to 2.36 at 200 rpm, and then slightly decreases at higher speeds. The combination of higher current and lower speed results in the lowest transmissibility values, indicating optimal damping performance. At 150 rpm and 0.8 A, the transmissibility is 0.62, the lowest value in the table, indicating excellent damping performance as shown in Figure 11–13.



**Figure 10.** Transmissibility v/s speed for sample 2

**Table 4.** Transmissibility of damper for sample 3

Speed (rpm)	Current (A)							
	0.1	0.2	0.3	0.4	0.5	0.6	0.7	0.8
150	1.86	1.78	1.45	1.27	1.225	1.21	0.67	0.62
160	1.98	1.88	1.62	1.38	1.34	1.26	0.69	0.63
170	2.06	1.96	1.78	1.52	1.46	1.34	0.71	0.64
180	2.18	2.04	1.96	1.64	1.56	1.41	0.73	0.68
190	2.29	2.16	2.08	1.71	1.64	1.44	0.75	0.72
200	2.36	2.23	2.2	1.77	1.72	1.56	0.77	0.74
210	2.28	2.14	2.02	1.62	1.61	1.41	0.75	0.73
220	2.14	2.03	1.84	1.54	1.54	1.34	0.74	0.72
230	2.02	1.84	1.72	1.44	1.42	1.22	0.73	0.72
240	1.91	1.72	1.64	1.36	1.34	1.16	0.72	0.71
250	1.84	1.64	1.46	1.32	1.22	1.12	0.71	0.71

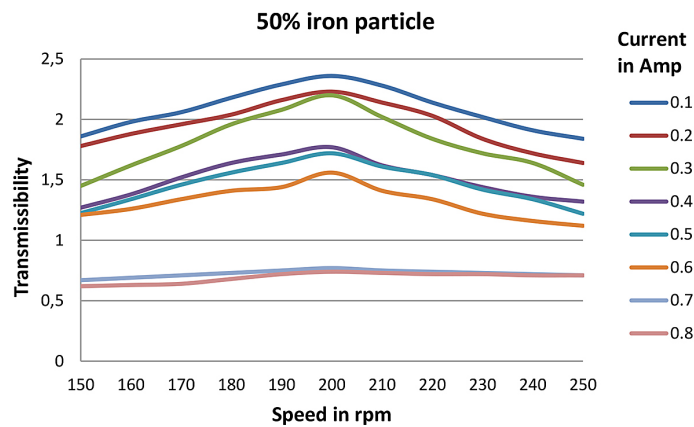


**Figure 11.** Transmissibility v/s speed for sample 3

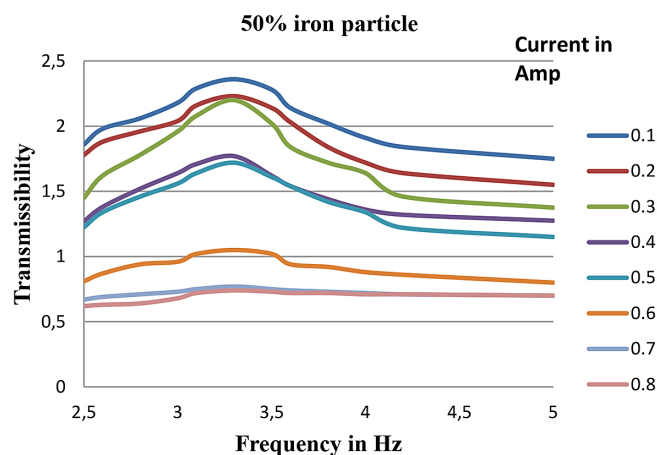


**Figure 12.** Transmissibility v/s frequency

**Comparison of MR and standard dampers**

*Effect of MR damper with 50% iron particle content*

At lower currents (0.1 A to 0.3 A), the transmissibility is higher, peaking around 3.5 Hz. As the

current increases, the transmissibility decreases, indicating better damping performance. Higher currents (above 0.5 A) show a significant reduction in transmissibility, suggesting stronger damping. The MR effect is more pronounced at increased currents,

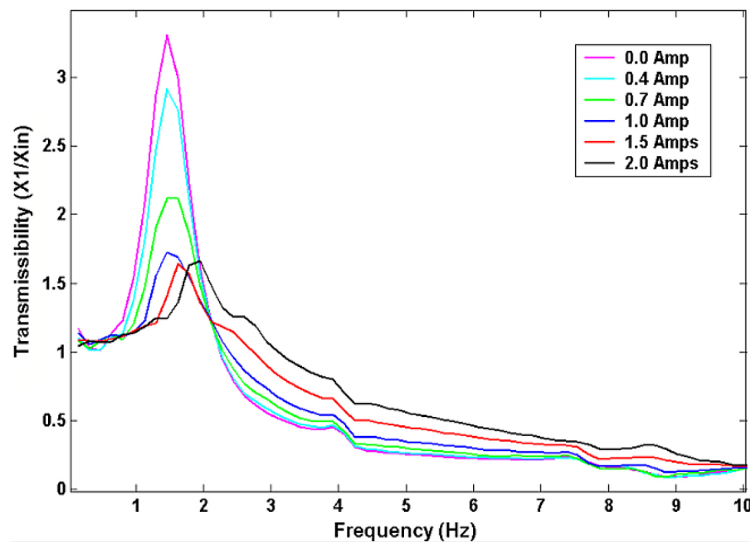


Figure 13. Transmissibility of Lord ML-430 MR damper

Table 5. Comparison of MR damper with standards Lord MR damper

Feature	Graph 1 (50% iron particle)	Graph 2 (higher current levels)
Frequency range	2.5–5 Hz	0–10 Hz
Current levels	0.1 A to 0.8 A	0.0 A to 2.0 A
Peak transmissibility	Around 2.0–2.2	Above 3.0 at low current (0.0 A)
Damping effect	Moderate, more effective above 0.5 A	Stronger, effective above 1.0 A
Overall performance	Effective in a narrow frequency range	More effective across a broader frequency range

effectively reducing the amplitude of vibrations. The frequency range is limited (2.5–5 Hz), making it suitable for analyzing specific vibration frequencies. The maximum transmissibility value reaches around 2.0–2.2 at lower currents, which indicates moderate vibration amplification at certain frequencies.

*Transmissibility vs. frequency for an MR damper at higher current levels*

The highest peak transmissibility (above 3.0) occurs at low current (0.0 A, 0.4 A, 0.7 A), particularly around 2 Hz. As current increases (above 1.0 A), the peak transmissibility is significantly reduced, indicating improved damping: Unlike the first graph, this one extends up to 10 Hz, allowing for a more comprehensive analysis of MR damper behavior. The damping effect is observed across a broader range of vibration frequencies, making it useful for applications with varying dynamic loads. At higher currents (1.5 A, 2.0 A), the transmissibility is consistently lower across all frequencies. This suggests that increasing current enhances the controllability and energy dissipation of the MR damper, effectively minimizing vibrations (Table 5).

- Graph 1 focuses on a specific iron particle composition (50%) in the MR fluid and a narrow frequency range, showing moderate damping performance.
- Graph 2 provides a more comprehensive analysis, showing the stronger damping effect at higher current values and across a wider frequency range.
- In both cases, increasing the current reduces the transmissibility, proving that MR dampers effectively control vibrations when properly energized.

**CONCLUSIONS**

The performance analysis confirms that MR dampers provide significant potential for vibration control in various applications, including structural and automotive systems. The damping force of the MR damper can be effectively tuned by adjusting the magnetic field strength, allowing real-time adaptability to dynamic loading conditions.

The transmissibility of the damper decreases as the applied current increases up to resonance (200 rpm), with the reduction in transmissibility ranging from 2.362 to 0.727. The 50% blend of iron particles in the MR fluid demonstrated the most effective damping performance, reducing transmissibility from 2.36 to 0.7475. The optimal damping force is achieved at a magnetic field current of 0.4 A; beyond this value, magnetic saturation occurs, reducing the damping effect. At resonance (200 rpm), the transmissibility for the 50% blend was observed to be 0.76 at 0.8 A, making it the most suitable choice for vibration attenuation.

The study confirms that the type and percentage of iron particles in the MR fluid significantly influence damping performance, with a 50% iron particle blend proving to be the optimal mixture for reducing vibration transmissibility.

### Acknowledgements

I would like to extend my heartfelt gratitude to Dr. Mrs. A.V. Patil, Director, School of Engineering, Management and research, Prof. Prabhat Ranjan, Vice Chancellor, D.Y. Patil International University, Pune for providing the resources and environment that supported this research. The authors confirm that they received no funding, grants or other provision to create this manuscript.

### REFERENCES

- Smith J., Wang L., & Johnson M. Design and experimental study of a novel magnetorheological damper with enhanced dynamic range. *Smart Materials and Structures*, 2021.
- Kumar A., Patel S., & Singh R. Adaptive control of vehicle suspension systems using magnetorheological dampers. *Journal of Vibration and Control*. 2022.
- Lee H., Cho K., & Park D. Seismic performance enhancement of structures with semi-active magnetorheological dampers. *Earthquake Engineering and Structural Dynamics*. 2023.
- Chen M., Zhao Y., & Huang L. Temperature-dependent behavior of magnetorheological dampers: Experimental analysis and modeling. *Journal of Intelligent Material Systems and Structures*. 2021.
- Gupta S., Verma P., & Sharma N. Development of a compact magnetorheological damper for prosthetic knee applications. *IEEE Transactions on Biomedical Engineering*. 2022.
- Nguyen T., Brown J., & Davis E. Modeling and control of magnetorheological dampers for vibration reduction in tall buildings. *Journal of Structural Engineering*. 2023.
- Martinez L., Rodriguez F., & Hernandez G. (Performance evaluation of magnetorheological dampers in offshore platform applications. *Ocean Engineering*. 2024.
- Singh K., Rao M., & Iyer V. A comparative study on control strategies for magnetorheological dampers in vehicle suspension systems. *Mechanical Systems and Signal Processing*. 2022.
- Kim D., Lee S., & Park J. (Integration of magnetorheological dampers in smart wearable devices for human motion assistance. *IEEE/ASME Transactions on Mechatronics*. 2023.
- Zhang Y., Li W., & Zhou Q. Real-time hybrid simulation of structures equipped with magnetorheological dampers. *Journal of Earthquake Engineering*. 2024.
- Huber M., Eschbach M., Kazerounian K., Ilies H. Functional evaluation of a personalized orthosis for knee osteoarthritis: A motion capture analysis. *J Med Devices Trans ASME*. 2021.
- Zuo Q., Zhao J.P., Mei X., Yi F., Hu G.L. Design and trajectory tracking control of a magnetorheological prosthetic knee joint. *Appl Sci Basel*. 2021.
- Lv H.Z., Sun Q., Zhang W.J. A comparative study of four parametric hysteresis models for magnetorheological dampers. *Actuators*. 2021.
- Rossi A., Orsini F., Scorza A., Botta F., Belfiore N.P., Sciuto S.A. A review on parametric dynamic models of magnetorheological dampers and their characterization methods. *Actuators*. 2018; 7: 16.
- Zhu X.C., Jing X.J., Cheng L. Magnetorheological fluid dampers: A review on structure design and analysis. *J Intell Mater Syst Struct*. 2012; 23: 839–73.
- Hu G.L., Zhang J.W., Zhong F., Yu L.F. Performance evaluation of an improved radial magnetorheological valve and its application in the valve-controlled cylinder system. *Smart Mater Struct*. 2019.
- Ioan B. Damper with magnetorheological suspension. *J Magn Magn Mater*. 2002; 241: 196–200.
- Ioan B. Magnetorheological suspension electromagnetic brake. *J Magn Magn Mater*. 2004
- Bai X.X., Hu W., Wereley N.M. Magnetorheological damper utilizing an inner bypass for ground vehicle suspensions. *IEEE Trans Magn*. 2013.
- Solepatil S., Awadhani L.V. Transmissibility analysis of magnetorheological damper. *Int J Latest Technol Eng Sci*. 2014; 1: 46–50.
- Solepatil S., Awadhani L.V. Effect of viscosity on a magnetorheological damper. *Int J Sci Res*. 2014; 1: 206–9.